Geophys. J. Int. (2007) **170,** 567–579 doi: 10.1111/j.1365-246X.2007.03487.x

Reflectivity method for geomechanical equilibria

Boris N. Kuvshinov

Shell International Exploration and Production B.V., PO Box 60, 2280AB *Rijswijk, The Netherlands. E-mail: Boris.Kuvshinov@shell.com*

Accepted 2007 May 3. Received 2007 February 28; in original form 2006 October 16

SUMMARY

It is shown that the block LU decomposition of the transfer and scattering matrix convert these matrices into each other. This allows to introduce a generalization of the Kennett reflectivity method, which is applicable to arbitrary systems of linear differential equations. The introduced method is convenient to analyse equilibria, where the governing matrix is degenerate. The resulting algorithm is compact and numerically stable. To illustrate the concept, we consider elastic equilibrium of a layered medium. We also derive closed-form expressions for a quasi-stationary poroelastic case taking into account solid–fluid and electrokinetic coupling.

Key words: elastic deformations, electrokinetic coupling, equilibrium,hydrocarbon reservoir, reflectivity method.

1 INTRODUCTION

Any change of fluid pore pressure inside a producing hydrocarbon reservoir induces deformations of the reservoir and of the surrounding formations. These deformations may influence the hydrocarbon flow and govern growth of fractures. They can also result in a number of undesired phenomena like sand production, or even borehole collapse. For these reasons, calculations of strains and stresses induced by extraction of hydrocarbons are of primary importance for reservoir engineering.

In this paper, we consider a semi-infinite medium, which consists of a number of horizontal layers with distinct material properties. The boundaries between the layers are called interfaces. The upper interface is the Earth surface. One of the layers contains fluid (hydrocarbons). We call this layer 'the reservoir layer' or simply 'the reservoir'. The pressure of fluid inside the reservoir changes due to hydrocarbon extraction. We assume that the pore pressure inside the reservoir is constant in the vertical direction, but it can vary in the horizontal plane. Our analysis is based on Biot's poroelasticity theory (Biot 1956) that describes coupled solid and fluid motion and equilibrium within the framework of linear elasticity.

Elastic deformations of a layered medium have been originally studied by Thomson (1950) and Haskell (1953), who developed a matrix formalism to describe propagation of elastic (seismic) waves. This formalism naturally leads to the propagator matrix method (Haskell 1964; Gilbert & Backus 1966). Ben-Menahem & Singh (1968) have developed a general approach to describe both static and dynamic elastic deformations. Using this approach Singh has introduced a propagator matrix method for static problems (Singh 1970). A similar formalism was presented independently by Sato (1971).

The major drawback of the propagator matrix method is that it deals with both decaying and growing exponents of $k_\perp h$, where $k_\perp$ is the absolute value of the horizontal wave vector and h is the layer thickness [strictly speaking these are hyperbolic sines, sinh $(k_\perp h)$, and cosines, cosh $(k_\perp h)$]. This usually leads to numerical instability. In case of elastic waves, the ill-conditioning of the propagator matrix method is overcome by working with reflection and transmission matrices rather than with wave amplitudes. Such an approach is called the reflectivity method. It has been developed by Fuchs (1968) and Fuchs & Müller (1971) for a layered medium without a free surface and a source located on one side of the layers. In a series of papers, Kennett and co-authors have applied the reflectivity method to the case of a half-space and a source with arbitrary depth (Kennett 1974; Kennett & Kerry 1979; Kennett 1983). Moreover, Kennett has partitioned the Thomson–Haskell propagator matrix into upward and downward reflection and transmission matrices for individual interfaces and layers, and has developed a recursive procedure to combine these matrices into global reflection and transmission matrices for a stack of layers. Only decaying exponents with the same scaling appear in calculations, so that Kennett's recursion procedure is numerically stable. The Kennett method has been subsequently generalized to anisotropic media (Booth & Crampin 1983; Fryer & Frazer 1984), and its modifications have been proposed (Rokhlin & Wang 2002). Currently, the reflectivity method is the most common tool in the theory of elastic wave propagating in layered media. Its detail description is given in reviews (Ursin 1983; Müller 1985) and monographs (see, e.g. Chapman 2004).

The Kennett method cannot be directly applied to the static case, because the standard decomposition of deformations on the primary and shear waves is inadequate at zero frequency (Takeuchi & Saito 1972). For this reason most of the studies of static deformations of a layered medium were dedicated to applications of the propagator matrix method or to its generalizations and modifications. Techniques to suppress numerical instability have been proposed in a number of references (Sato & Matsu'ura 1973; Jovanovich *et al.* 1974; Matsu'ura & Sato 1975; Wang 1999). The original propagator matrix method (Singh 1970) has been extended to describe a viscoelastic-gravitational case (Rundle 1980, 1981, 1982) and to obtain internal deformation fields (Roth 1990; Ma & Kusznir 1992). It has been also applied for earthquake and fault modelling (Singh *et al.* 1997; Savage 1998; Bonafede & Rivalta 1999; Singh & Singh 2004). A similar method based on Stroh formalism has been developed by Pan and co-authors (Pan 1997, 2001, 2003; Yang & Pan 2002) who have derived a number of Green's function in multilayered media. Other references on studies of static deformations of a layered media can be found in (Benitez & Rosakis 1987) and in more recent papers (Wang *et al.* 2003; Zhao *et al.* 2004; Fukahata & Matsu'ura 2005).

An alternative numerical scheme, which is frequently used to describe static deformations of a layered medium, is the so-called flexibility matrix method. It was originally introduced by Bufler (1971) and then developed by other authors (Linkov & Filippov 1991; Peirce & Siebrits 2001a,b). In the flexibility matrix method, stresses at the top and the bottom of the layers are expressed through displacements at the top and the bottom of the layers, or vice versa. By expressing stresses through displacements one obtains matrices, whose elements contain hyperbolic functions tanh $(k_\perp h)$ and $1/\cosh(k_\perp h)$, but not sinh $(k_\perp h)$ and cosh $(k_\perp h)$ as it was in the case of the propagator matrix. This avoids the numerical instability at large wave vectors or thick layers. At small wave vectors or thin layers the scheme becomes unstable. Thus, the flexibility matrix method shifts the numerical instability to a different range of parameters, but does not eliminate it. Ill-conditioning of both the propagator and flexibility matrix methods has been confirmed in numerical studies (Maier & Novati 1986, 1987).

Zhu & Rivera (2002) have noted that elasto-dynamic and elasto-static problems can be treated in a unified way using the Jordan decomposition of the matrix that determines the vertical dependence of deformations. It has been also shown that the Thomson–Haskell propagator matrix coincides with the Singh propagator matrix in the limit $\omega \to 0$. This suggests that an equilibrium can be considered as a wave with zero frequency ω. The difficulty of this approach is that one has to deal with uncertainties of the type '0/0', since the eigenvalues of the propagator matrix merge at $\omega \to 0$. The above difficulty can be overcome by constructing a modified reflectivity method, where the static solution is used explicitly to perform matching across the layers (Xie & Yao 1989; He *et al.* 2003). However, this results in cumbersome relations, which do not have apparent connection with the original Kennett procedure.

In this paper, we combine ideas of Xie & Yao (1989), He *et al.* (2003) and Zhu & Rivera (2002) to develop a general and compact reflectivity scheme to analyse static equilibria of a layered medium. We note that although the original reflectivity method has been developed for the wave equation (Fuchs & Müller 1971; Kennett 1974), it has in fact a much wider scope of applicability. The notions of reflection and transmission matrices can be introduced for arbitrary vectors, whose values at different points are linearly related. These reflection and transmission matrices obey the usual composition rules, which allows us to calculate them using the Kennett recursion procedure. In this formulation the reflectivity method becomes a purely algebraic scheme that does not depend on the underlying physics. There exists a formal difference between the dynamic and static cases. In the dynamic case, the governing matrix can be fully diagonalized and reduced to the eigenvalue matrix. In the static case, the governing matrix is partially diagonalized and is represented in the Jordan canonical form. From the point of view of the reflectivity method it means, that the transmission matrices through individual layers are equal to exponents of the Jordan canonical matrices, rather than to exponents of eigenvalue matrices. Taking this circumstance into account and introducing proper reflection and transmission matrices at interfaces, one obtains a scheme that is applicable to arbitrary static equilibria.

2 DESCRIPTION OF THE APPROACH

2.1 Specifics of the problem

Linear equilibrium of an elastic, horizontally layered medium is described by a system of equations of the form

$$\frac{\partial \vec{\psi}}{\partial z} = \hat{\mathbf{A}} \cdot \vec{\psi} + \vec{F}. \tag{1}$$

Here, the vector $\vec{\psi}$ is a set of physical parameters characterizing the medium, $\vec{F}$ represents an external force, z is the vertical coordinate, and $\hat{\mathbf{A}}$ is the governing matrix. Concrete expressions for $\vec{\psi}$, $\hat{\mathbf{A}}$, and $\vec{F}$ depend on the type of equilibrium. In what follows we assume that $\vec{\psi}$ is continuous everywhere. The values of $\hat{\mathbf{A}}$ and $\vec{F}$ are constant within a given layer, but they can vary through interfaces.

For wave-type equations, system (1) has an even dimension $2n$, since each upward wave has a counterpart travelling downwards. The matrix $\hat{\mathbf{A}}$ is generally speaking non-degenerate and it has $2n$ distinct eigenvalues λ_j and eigenvectors or eigenmodes $\vec{\boldsymbol{m}}_j$. The basic idea behind the reflectivity method is to describe wave propagation in terms of transmission and reflection matrices for above eigenmodes.

The matrix $\hat{\mathbf{A}}$ becomes degenerate in the stationary limit. Appearance of this degeneracy can be seen from physical reasoning. Consider, for example, purely elastic waves. As is well known, there exist two types of such waves, that is, the primary and shear waves, which satisfy the dispersion relations $\omega^2 = k^2 C_P^2$ and $\omega^2 = k^2 C_S^2$. Here, ω is the wave frequency, k is the wave vector, C_P and C_S are phase velocities. The eigenvalues of the corresponding matrix $\hat{\mathbf{A}}$ are equal to $\lambda = \pm(k_\perp^2 - k^2)^{1/2}$, where $k_\perp$ is the horizontal wave vector. The primary and shear waves with a given frequency have different values of k^2. Consequently, there exist four different eigenvalues λ for each $k_\perp$. Two dispersion relations merge to $k^2 = 0$ in the limit $\omega \to 0$, and only two eigenvalues $\lambda = \pm k_\perp$ remain.

If one the eigenvalue λ is degenerate, it is possible to construct only one corresponding eigenvector which depends on the vertical coordinate z as $\exp(\lambda z)$. The other linearly independent solutions corresponding to the same λ vary with the vertical coordinate z as $\vec{\psi} \propto (\vec{\psi}_0 + \vec{\psi}_1 z + \vec{\psi}_2 z^2 + \ldots)\ \exp(\lambda z)$. The constant vectors $\vec{\psi}_j$ can be found explicitly by substituting solutions of the above form in eq. (1). Such an approach, however, is rather tedious.

2.2 Jordan decomposition

To write down solution of eq. (1) in a compact form, we use the Jordan decomposition of the matrix $\hat{\mathbf{A}}$: $\hat{\mathbf{A}} = \boldsymbol{M} \cdot \boldsymbol{J} \cdot \boldsymbol{M}^{-1}$. Here, the columns of the matrix $\boldsymbol{M}$ are generalized eigenvectors of $\hat{\mathbf{A}}$, and $\boldsymbol{J}$ is a block-diagonal matrix, consisting of blocks $\boldsymbol{J}_j$. Each of these blocks is associated with a given eigenvalue λ_j of $\hat{\mathbf{A}}$ and it has the properties,

$$\boldsymbol{J}_j = \begin{pmatrix} \lambda_j & 1 & & 0 \\ 0 & \lambda_j & 1 & \\ & \ddots & \ddots & \ddots \\ 0 & & & \lambda_j \end{pmatrix}, \tag{2}$$

and

$$e^{\boldsymbol{J}_j\zeta} = e^{\lambda_j\zeta}\begin{pmatrix} 1 & \zeta & \cdots & \frac{\zeta^{D-1}}{(D-1)!} \\ & \ddots & \ddots & \\ & & 1 & \zeta \\ 0 & & & 1 \end{pmatrix}, \tag{3}$$

where D is the dimension of $\boldsymbol{J}_j$. The matrix exponential $\exp(\hat{\mathbf{A}}\zeta)$ has a block-diagonal form, consisting of $\exp(\boldsymbol{J}_j\,\zeta)$. There are D generalized eigenvectors associated with λ_j. The first of these vectors $\vec{\boldsymbol{m}}_1^{(j)}$ is the usual eigenvector of the matrix $\hat{\mathbf{A}}$, which satisfies the condition $\hat{\mathbf{A}}\cdot\vec{\boldsymbol{m}}_1^{(j)} = \lambda_j\vec{\boldsymbol{m}}_1^{(j)}$. The other vectors are constructed recursively, by solving the equation $\hat{\mathbf{A}}\cdot\vec{\boldsymbol{m}}_{l+1}^{(j)} = \lambda_j\vec{\boldsymbol{m}}_{l+1}^{(j)}+\vec{\boldsymbol{m}}_l^{(j)}$, $l = 1, \ldots, D-1$. We group together the generalized eigenvectors associated with eigenvalues $\lambda_1, \lambda_2, \ldots$, whose real part is positive, to compose the submatrix $\boldsymbol{M}^{(+)} = (\vec{\boldsymbol{m}}_1^{(1)}, \vec{\boldsymbol{m}}_2^{(1)}, \ldots, \vec{\boldsymbol{m}}_1^{(2)}, \vec{\boldsymbol{m}}_2^{(2)}, \ldots)$. The submatrix $\boldsymbol{M}^{(-)}$ is composed in a similar manner from generalized eigenvectors associated with negative eigenvalues. The generalized eigenvector matrix $\boldsymbol{M}$ and the solution of eq. (1) in the absence of external forces are then written as $\boldsymbol{M} = (\boldsymbol{M}^{(+)}, \boldsymbol{M}^{(-)})$ and

$$\vec{\psi} = \boldsymbol{M}\cdot\vec{\boldsymbol{C}}, \qquad \vec{\boldsymbol{C}}(z) = e^{\boldsymbol{J}(z-z_0)}\cdot\boldsymbol{M}^{-1}\cdot\vec{\psi}(z_0). \tag{4}$$

Components of the vector $\vec{\boldsymbol{C}}$ are the amplitudes of eigenmodes. They are also referred to as the spectral coefficients (Peirce & Siebrits 2001a,b).

2.3 Reflectivity method

The key circumstance for the further analysis is that the reflectivity method can be viewed as an abstract algebraic scheme. Suppose there exists a linear translation rule that relates components of arbitrary $2n$-dimensional vectors $\vec{\boldsymbol{V}}$ in two points a and b as

$$\vec{\boldsymbol{V}}(b) = \boldsymbol{Q}(b, a)\cdot\vec{\boldsymbol{V}}(a). \tag{5}$$

The arguments of the transfer matrix $\boldsymbol{Q}$ are read from right to left, that is, $\boldsymbol{Q}\,(b, a)$ propagates vectors $\vec{\boldsymbol{V}}$ from point a to point b. One partitions $\boldsymbol{Q}$ in four $(n\times n)$-blocks and factor it into product of two matrices,

$$\boldsymbol{Q}(b, a) = \boldsymbol{L}^{-1}(a, b)\cdot\boldsymbol{U}(b, a), \tag{6}$$

where

$$\boldsymbol{L}(a, b) = \begin{bmatrix}\boldsymbol{T}(a, b) & 0 \\ -\boldsymbol{R}(a, b) & \boldsymbol{I}\end{bmatrix}, \quad \boldsymbol{U}(b, a) = \begin{bmatrix}\boldsymbol{I} & -\boldsymbol{R}(b, a) \\ 0 & \boldsymbol{T}(b, a)\end{bmatrix}, \tag{7}$$

and $\boldsymbol{I}$ is the unit matrix. This representation is the usual block LU decomposition of the matrix $\boldsymbol{Q}$. The fact that we write $\boldsymbol{L}^{-1}$ rather than $\boldsymbol{L}$ does not play a role, because the matrices $\boldsymbol{L}$ and $\boldsymbol{U}$ have the same block structure as their inverses. We also partition $\vec{\boldsymbol{V}}$ in upper and lower parts, $\vec{\boldsymbol{V}} = (\vec{\boldsymbol{V}}_u, \vec{\boldsymbol{V}}_d)^T$, and treat these parts as signals propagating 'upwards' and 'downwards'. If one assumes that point b lies 'below' and point a lies 'above', then eq. (5) with the matrix $\boldsymbol{Q}(b, a)$ given by eqs (6) and (7) has the same form as relations describing signal transmissions and reflections. The matrices $\boldsymbol{T}$ and $\boldsymbol{R}$ play the role of transmission and reflection matrices for a signal, which propagates in the direction indicated by arguments of these matrices. One concludes, that $\boldsymbol{T}$ and $\boldsymbol{R}$ for a combined path '$a\to b\to c$' satisfy the standard 'transmission/reflection' composition rules (Kennett 1983),

$$\boldsymbol{T}(a, c) = \boldsymbol{T}(a, b)\cdot[\boldsymbol{I} - \boldsymbol{R}(c, b)\cdot\boldsymbol{R}(a, b)]^{-1}\cdot\boldsymbol{T}(b, c), \tag{8}$$

$$\boldsymbol{R}(a, c) = \boldsymbol{R}(b, c) + \boldsymbol{T}(c, b)\cdot\boldsymbol{R}(a, b)\cdot[\boldsymbol{I} - \boldsymbol{R}(c, b)\cdot\boldsymbol{R}(a, b)]^{-1}\cdot\boldsymbol{T}(b, c). \tag{9}$$

Relations for $\boldsymbol{T}(c, a)$ and $\boldsymbol{R}(c, a)$ are obtained by interchanging the arguments $a\leftrightarrow c$ in eqs (8) and (9). Above equations can be also verified by direct calculation. Their mathematical meaning is transparent: they express the block LU decomposition of a matrix product in terms of LU decompositions of individual matrices.

2.4 Computational scheme

Eq. (4) provides a translation rule for the vector $\vec{\boldsymbol{C}}$. Translation between points z_0 and z within a single layer is given by $\vec{\boldsymbol{C}}(z) = \exp[\boldsymbol{J}(z-z_0)]\cdot\vec{\boldsymbol{C}}(z_0)$. If points z_0 and z are separated by an interface, then $\vec{\boldsymbol{C}}(z) = \boldsymbol{M}^{-1}(z)\cdot\boldsymbol{M}(z_0)\cdot\vec{\boldsymbol{C}}(z_0)$. We apply the formalism of Section 2.3 to the above translation rule. Without loss of generality we label the points in such a way that $z > z_0$ and assume that the z-axis is directed upwards.

The LU decomposition of the form of eqs (6) and (7) has a duality property. Namely, blocks of $\boldsymbol{Q}(b, a)$ are elements of the LU decomposition for a matrix $\boldsymbol{S}$ composed from the reflection and transmission matrices,

$$\underbrace{\begin{bmatrix}\boldsymbol{T}(a, b) & \boldsymbol{R}(b, a) \\ \boldsymbol{R}(a, b) & \boldsymbol{T}(b, a)\end{bmatrix}}_{=\boldsymbol{S}} = \begin{pmatrix}\boldsymbol{Q}_{11} & 0 \\ -\boldsymbol{Q}_{21} & \boldsymbol{I}\end{pmatrix}^{-1}\cdot\begin{pmatrix}\boldsymbol{I} & -\boldsymbol{Q}_{12} \\ 0 & \boldsymbol{Q}_{22}\end{pmatrix}. \tag{10}$$

The first matrix subscript enumerates rows and the second one enumerates columns, so that $\boldsymbol{Q}_{12}$ is the upper-right subblock of $\boldsymbol{Q}(b, a)$. The matrix $\boldsymbol{S}$ in Eq. (10) is the same as the S-matrix in scattering theory with interchanged blocks ($\boldsymbol{R}$-blocks stand on the diagonal of the S-matrix). This difference appears, because in scattering theory one relates ingoing and outgoing waves at interfaces, rather than waves propagating in fixed directions. eq. 10) is convenient to obtain LU decomposition of arbitrary matrices. In particular, by applying it to the Jordan matrix one has

$$e^{\boldsymbol{J}(z-z_0)} = \begin{bmatrix}e^{-\boldsymbol{J}_+(z-z_0)} & 0 \\ 0 & \boldsymbol{I}\end{bmatrix}^{-1}\cdot\begin{bmatrix}\boldsymbol{I} & 0 \\ 0 & e^{\boldsymbol{J}_-(z-z_0)}\end{bmatrix}, \tag{11}$$

where $\boldsymbol{J}_+$ and $\boldsymbol{J}_-$ are the upper and lower blocks of $\boldsymbol{J}$. By construction, the blocks $\boldsymbol{J}_+$ and $\boldsymbol{J}_-$ contain positive and negative eigenvalues correspondingly, so that the layer transmission matrices, $\boldsymbol{T}(z, z_0) = \exp[\boldsymbol{J}_-(z-z_0)]$ and $\boldsymbol{T}(z_0, z) = \exp[-\boldsymbol{J}_+(z-z_0)]$, exponentially decay in both directions. The layer reflection matrices are equal to zero. The transmission and reflection matrices for interfaces are found by decomposing the matrix $\boldsymbol{M}^{-1}(z)\cdot\boldsymbol{M}(z_0)$. Once the reflection and transmission matrices for individual layers and interfaces are determined, one proceeds in the same way as in the standard Kennett method. The numerical stability is achieved because decomposition (11) separates solutions with different exponents.

It is possible to formulate the reflectivity scheme in terms of the vector $\vec{\psi}$. The translation rule for this vector is given by a sequence of transfer matrices $\boldsymbol{Q}(z, z_0) = \boldsymbol{M}(z)\cdot\exp[\boldsymbol{J}(z-z_0)]\cdot\boldsymbol{M}^{-1}(z_0)$. One needs to decompose each of the three matrices in this expression according to eq. (7) and then recursively calculate transmissions and reflections through stack of layers using eqs (8) and (9). The difference with the standard approach is that the eigenvector matrices $\boldsymbol{M}$ and $\boldsymbol{M}^{-1}$ are decomposed individually. A scheme of this type for seismic waves has been presented by Rokhlin & Wang (2002).

3 STATIONARY DEPLETING RESERVOIR

In this section, we consider a stationary depleting reservoir to illustrate the introduced concept. A more complicated example is given in Appendix A.

3.1 Elastostatic equilibrium

The poroelastic reservoir equilibrium should be found by solving coupled momentum balance equations for the solid frame and the pore fluid. The solid and fluid equilibria are decoupled at characteristic times t and lengths l such as $l^2/t \ll D_p$, where D_p is the diffusion coefficient of the pore fluid pressure. In notations of Appendix A the above condition reads as $\chi/H_p \ll 1$. When this condition is satisfied, then one deals with a stationary elastostatic problem. Its solution is obtained by considering the limit $\partial/\partial t = 0$ of equations given in Appendix A or of equations derived by Wang & Kümpel (2003), and it is written as

$$\underbrace{\begin{pmatrix} \nabla\cdot\hat{\boldsymbol{u}}_\perp \\ \hat{\tau}_{zz} \\ \frac{\nabla\cdot\hat{\vec{\boldsymbol{\tau}}}_{\perp z}}{k_\perp} \\ k_\perp \hat{u}_z \end{pmatrix}}_{=\vec{\psi}} = \underbrace{\begin{pmatrix} 1 & \mu & 1 & -\mu \\ -2N & N & -2N & -N \\ 2N & N & -2N & N \\ -1 & \mu & 1 & \mu \end{pmatrix}}_{=\boldsymbol{M}} \cdot \vec{\boldsymbol{C}} - \underbrace{\frac{\alpha \hat{p}_f}{H_d} \begin{pmatrix} -1 \\ 2N \\ 0 \\ 0 \end{pmatrix}}_{=\vec{\psi}_{\text{part}}}. \tag{12}$$

Here, $k_\perp$ is the 'wave vector' in the horizontal plane, hats denote transformed variables, and the other parameters are explained in Appendix A. We did not specify the type of transform to derive eq. (12) and defined the wave vector formally in terms of transformed Laplacian, $\nabla_\perp^2 \to -k_\perp^2$. Exact meaning of $k_\perp$ is different for Fourier transform, Hankel transform, and discrete Fourier transform. The matrix $\boldsymbol{M}$ in eq. (12) is composed from corresponding components of vectors $\vec{\boldsymbol{m}}_{1,2}$, see eqs (A18)–(A20), (A22). The terms with $\bar{\alpha}$ in expressions for $\vec{\boldsymbol{m}}_2$ (A20), (A22) are omitted, because they are incorporated in the vector $\vec{\boldsymbol{m}}_1$. In contrast to the general poroelastic case, the distribution of the pore pressure p_f is assumed to be known, and it plays a role of an external force. The term $\vec{\psi}_{\text{part}}$ represents a response of the solid frame on this force. It is found from first two eqs (A15) by setting $\partial^2/\partial\hat{z}^2 = 0$ there.

The elastostatic system has two eigenvalues $\lambda = \pm k_\perp$, so that its Jordan matrix consists of two (2×2)-blocks of type (2). The transmission matrices through layers are determined by eq. (11): $\boldsymbol{T}^U = \exp(-\boldsymbol{J}_+ h)$ and $\boldsymbol{T}^D = \exp(\boldsymbol{J}_- h)$, where h is the layer thickness. To find the transmission and reflection matrices through interfaces we take point a just above an interface and point c just below the same interface and apply eq. (10) to the matrix $\boldsymbol{Q}(c, a) = \boldsymbol{M}^{-1}(c) \cdot \boldsymbol{M}(a)$. This gives

$$\boldsymbol{T}^U(a, c) = 2N_c(1 - \nu_c) \begin{pmatrix} \frac{1}{N_c/2 + \mu_c N_a} & 0 \\ 0 & \frac{1}{\mu_a N_c + N_a/2} \end{pmatrix}, \tag{13}$$

and

$$\boldsymbol{R}^U(a, c) = \begin{pmatrix} 0 & \frac{1}{2}\frac{\mu_a N_c - \mu_c N_a}{\mu_a N_c + N_a/2} \\ \frac{N_a - N_b}{N_c/2 + \mu_c N_a} & 0 \end{pmatrix}. \tag{14}$$

The upward transmission and reflection matrices are given by the expressions,

$$\boldsymbol{T}^D(c, a) = \boldsymbol{T}^U(c, a), \qquad \boldsymbol{R}^D(c, a) = -\boldsymbol{R}^U(c, a). \tag{15}$$

Notations $\boldsymbol{T}^U(c, a)$ and $\boldsymbol{R}^U(c, a)$ mean that one should formally apply eqs (13) and (14) with interchanged arguments $a \leftrightarrow c$.

3.2 Matching through reservoir

The remaining procedure is similar to calculation of the response from a buried seismic source. Starting form the horizontal level $z = z_s$ just above the surface, and from the level $z = z_\infty$ just below the lowermost interface, and applying eqs (8) and (9) recursively, one calculates $\boldsymbol{R}^U(\text{'}t\text{'}, z_s)$ and $\boldsymbol{R}^D(\text{'}b\text{'}, z_\infty)$. Here, '$t$' and '$b$' label levels just outside the reservoir top and bottom. As the result, the original multi-layer boundary value problem is reduced to a single layer boundary problem, which can be solved analytically.

Components of $\vec{\psi}$ in eq. (12) have been chosen in such a way that they are continuous everywhere. The reservoir differs from the other layers by presence of the term $\vec{\psi}_{\text{part}}$. Continuity of $\vec{\psi}$ implies the matching condition

$$\boldsymbol{M} \cdot \vec{\boldsymbol{C}}|_{\text{res}} + \vec{\psi}_{\text{part}} = \boldsymbol{M} \cdot \vec{\boldsymbol{C}}|_{\text{out}}. \tag{16}$$

The subscripts '*res*' and '*out*' refer to points inside and outside the reservoir. In solving eq. (16) one can assume that the reservoir and the neighbouring layers have the same material properties. If this is not the case, such layers are introduced artificially. This does not influence the result, provided the thickness of the introduced layers is sufficiently small. The reflection matrices $\boldsymbol{R}^U(\text{'}t\text{'}, z_s)$ and $\boldsymbol{R}^D(\text{'}b\text{'}, z_\infty)$, relate components $\vec{\boldsymbol{C}}_u$ and $\vec{\boldsymbol{C}}_d$ of the partitioned vector $\vec{\boldsymbol{C}}$ at points 't' and 'b' as

$$\vec{\boldsymbol{C}}_d(\text{'}t\text{'}) = \boldsymbol{R}^U(\text{'}t\text{'}, z_s) \cdot \vec{\boldsymbol{C}}_u(\text{'}t\text{'}), \tag{17}$$

$$\vec{\boldsymbol{C}}_u(\text{'}b\text{'}) = \boldsymbol{R}^D(\text{'}b\text{'}, z_\infty) \cdot \vec{\boldsymbol{C}}_d(\text{'}b\text{'}). \tag{18}$$

Applying eq. (16) to the top and bottom reservoir boundaries and solving it together with eqs (17) and (18) one has

$$\vec{\boldsymbol{C}}_u(\text{'}t\text{'}) = \left(\boldsymbol{I} - \boldsymbol{W}^D \cdot \boldsymbol{W}^U\right)^{-1} \cdot \left(\boldsymbol{I} + \boldsymbol{W}^D\right) \cdot \vec{\boldsymbol{\pi}}, \tag{19}$$

$$\vec{\boldsymbol{C}}_d(\text{'}b\text{'}) = \left(\boldsymbol{I} - \boldsymbol{W}^U \cdot \boldsymbol{W}^D\right)^{-1} \cdot \left(\boldsymbol{I} + \boldsymbol{W}^U\right) \cdot \vec{\boldsymbol{\pi}}. \tag{20}$$

Here, $\boldsymbol{T}^{U,D}_{\text{res}}$ are the transmission matrices through the reservoir

$$\vec{\boldsymbol{\pi}} = \frac{\alpha \hat{p}_f}{2H_d} \begin{pmatrix} 1 - e^{-k_\perp h_{\text{res}}} \\ 0 \end{pmatrix}, \tag{21}$$

h_{res} is the reservoir thickness, and

$$\boldsymbol{W}^U = \boldsymbol{T}^D_{\text{res}} \cdot \boldsymbol{R}^U(\text{'}t\text{'}, z_s), \qquad \boldsymbol{W}^D = \boldsymbol{T}^U_{\text{res}} \cdot \boldsymbol{R}^D(\text{'}b\text{'}, z_\infty). \tag{22}$$

Eqs (17)–(20) define the total vector $\vec{\boldsymbol{C}}$ at points 't' and 'b'. Starting from these points one translates $\vec{\boldsymbol{C}}$ upwards and downwards, which determines elastic deformations everywhere in space.

3.3 Subsidence and compaction

Lets interpret eq. (12) as the Fourier transform. The value of a function in the k-space at $k_\perp \to 0$ is equal to the integral of the original function in the coordinate space over the horizontal (x, y)-plane. In particular, $\hat{u}_z(z)$ at $k_\perp \to 0$ is equal to the total displaced volume at the level z. From equations of Section 3.2 it follows that the reservoir layer, that is, the whole layer restricted by the horizontal planes at the reservoir top and bottom, has the volume change of ΔV_{res},

$$\Delta V_{\text{res}} = \frac{\alpha h_{\text{res}}}{H_d} \int p_f(\vec{r}_\perp)\, d\vec{r}_\perp. \tag{23}$$

The pressure decreases due to hydrocarbon production, $p_f < 0$, and $\Delta V_{\rm res}$ is negative. Eq. (23) states that the reservoir compacts as a 1-D medium with the 'uni-axial' compressibility coefficient $C_u = 1/H_d$. Volumes of non-reservoir layers do not change, because the layer transmission matrix turns to a unit matrix in the limit $k_\perp \to 0$.

The transmission and reflection matrices between any two non-reservoir layers are the same as if these two layers were adjacent. Indeed, the transfer matrix between interfaces at z_n and z_1 is equal to $\boldsymbol{Q}(z_n, z_1) = \boldsymbol{M}^{-1}(z_n) \cdot \boldsymbol{M}(z_{n-1}) \cdot \boldsymbol{I} \cdot \boldsymbol{M}^{-1}(z_{n-1}) \cdot \ldots \cdot \boldsymbol{M}(z_1) = \boldsymbol{M}^{-1}(z_n) \cdot \boldsymbol{M}(z_1)$. Consequently, the matrix $\boldsymbol{R}^U(\text{'}t\text{'}, z_s)$ depends only on elastic properties of the reservoir and of the uppermost layer, while the matrix $\boldsymbol{R}^D(\text{'}b\text{'}, z_\infty)$ depends only on elastic properties of the reservoir and of the lowermost layer. The uppermost most layer is atmosphere, which can be treated as an infinitely soft material. From eq. (14) it follows

$$\boldsymbol{R}^U(\text{'}t\text{'}, z_s) = \begin{pmatrix} 0 & 1/2 \\ -2 & 0 \end{pmatrix}. \tag{24}$$

If the lowermost layer is infinitely rigid, then the subsidence volume above the reservoir is equal to the reservoir compaction (23). If the lowermost layer has the same elastic properties as the reservoir, then $\boldsymbol{R}^D(\text{'}b\text{'}, z_\infty) = 0$. Applying equations of Section 3.2 to this case, one finds the subsidence volume above the reservoir,

$$V_{\rm sub} = -2(1-\nu)\,\Delta V_{\rm res}. \tag{25}$$

Eq. (25) has been derived by Geertsma (1973), who has analysed an infinitely thin cylindrical reservoir in a uniform semi-space. We see that this equation does not depend on the reservoir thickness and it is also valid, if intermediate non-reservoir layers are added.

3.4 Displacement of reservoir bottom

From eqs (23) and (25) we see that the total volumetric displacements of the reservoir bottom $V_{\rm bot}$ is equal to $V_{\rm bot} = V_{\rm sub} - \Delta V_{\rm res} = -(1-2\nu)\, V_{\rm res}$. Since the Poisson ratio ν is always less than 0.5, the horizontal level at the reservoir bottom moves in average in the same direction as the Earth surface and the reservoir top, that is, downwards if the reservoir is depleting. This means that the layered half-space model does not recover exactly the limiting case of an infinite space, even if the free surface is placed at infinity. Due to symmetry of the problem, the top and the bottom of a depleting reservoir in a uniform infinite space move towards each other, which contradicts the above conclusion.

To get a better idea of what happens in a half-space we consider the Geertsma model (Geertsma 1973; Segall 1992). The vertical displacement u_z near the axis of a uniformly depleted, cylindrical reservoir is given by the equation

$$u_z(z) = \bar{u}_z \left[\operatorname{sign}(d-z)\left(1 - \frac{\zeta_-}{\sqrt{1+\zeta_-^2}}\right) + (3-4\nu)\left(1 - \frac{\zeta_+}{\sqrt{1+\zeta_+^2}}\right) - \frac{2z}{r_{\rm res}} \frac{1}{(1+\zeta_+^2)^{3/2}} \right], \tag{26}$$

which is obtained by taking the limit $r/r_{\rm res} \ll 1$ in Geertsma's formulas. Here, $\zeta_\pm = |d \pm z|/r_{\rm res}$, $\bar{u}_z = -\alpha p_f h_{\rm res}/(2H_d)$, $r_{\rm res}$ and d are the reservoir radius and depth. The z-axis is directed downwards and $z = 0$ at the surface, which implies that for downward displacement the value u_z is positive. At depth $z \simeq d$ one has $\zeta_- \simeq 0$ and $\zeta_+ \simeq 2d/r_{\rm res}$. According to eq. (26), the central part of the reservoir bottom moves down, $u_{z,bot} \simeq 2(1-2\nu)\bar{u}_z$, for shallow reservoirs with $d/r_{\rm res} \ll 1$, and it moves up, $u_{z,bot} \simeq -\bar{u}_z$, for deep reservoirs with $d/r_{\rm res} \gg 1$. In case of shallow reservoirs, the total displaced volume at the reservoir bottom is evaluated by multiplying $u_{z,bot}$ on the reservoir area, $V_{bot} = \pi r_{\rm res}^2 u_{z,bot} = 2\pi r_{\rm res}^2 (1-2\nu)\bar{u}_z$. This value of $V_{\rm bot}$ agrees with the above analysis. A paradox appears in case of deep reservoirs—in spite of the fact that the central part of the bottom moves up, the value $V_{\rm bot}$ remains the same as in case of shallow reservoirs. To explain this paradox one should take into account points lying at large distances from the reservoir axis. These points have infinitesimally small downward displacements. However, they occupy an infinite area, so that their cumulative effect is finite and it eventually determines the value of $V_{\rm bot}$. This is illustrated by Fig. 1.

Although we have formally resolved the paradox, the practical question concerning the actual subsidence volumes cannot be always answered. In order to retrieve the 'correct' value of $V_{\rm bot}$ one might need to go such large distances, where the applicability of the underlying model is violated.

4 BI-MATERIAL FORMATIONS

Below we calculate displacements and stresses in a formation composed of two different materials. We assume that material '0' lays on the top of the second material. The reservoir layer is located inside the second material on the distance of d from the interface. Like in the above example with the cylindrical reservoir, the vertical z-axis is directed downwards, and $z = 0$ at the interface. In Section 4.1 it is demonstrated that the developed formalism allows to obtain known analytical results in a simple and unified way. A numerical example to validate the method is given in Section 4.2.

4.1 Nucleus of strain

Propagating the reflection matrix $\boldsymbol{R}^U$ downwards one finds

$$\boldsymbol{R}^U(z_s, z) = \exp(-2\hat{z}) \begin{pmatrix} -s_0\hat{z} & q_0 + s_0\hat{z}^2 \\ -s_0 & s_0\hat{z} \end{pmatrix}. \tag{27}$$

Here, $\hat{z} = k_\perp z$, z is the vertical coordinate of any point above the reservoir,

$$s_0 = \frac{N - N_0}{N/2 + \mu N_0}, \qquad q_0 = \frac{1}{2}\frac{\mu_0 N - \mu N_0}{\mu_0 N + N_0/2}. \tag{28}$$

Values without subscripts refer to the reservoir material and values with the subscript '0' refer to the non-reservoir material. The reflection matrix $\boldsymbol{R}^D(\text{'}b\text{'}, z_\infty)$ vanishes. From eq. (19) it then follows that $\vec{\boldsymbol{C}}_u(\text{'}t\text{'}) = \vec{\boldsymbol{\pi}}$. The value $\vec{\boldsymbol{C}}_u(z)$ everywhere above the reservoir is found by applying the upward propagating matrix to the vector $\vec{\boldsymbol{C}}_u(\text{'}t\text{'})$, that is, $\vec{\boldsymbol{C}}_u(z) = \boldsymbol{T}^U(z, d) \cdot \vec{\boldsymbol{\pi}}$. The value $\vec{\boldsymbol{C}}_d(z)$ is equal to $\vec{\boldsymbol{C}}_d(z) = \boldsymbol{R}^U(z_s, z) \cdot \vec{\boldsymbol{C}}_u(z)$.

For clarity, we consider the case of a thin reservoir, where $k_\perp h_{\rm res} \ll 1$ and $1 - \exp(-k_\perp h_{\rm res}) \simeq k_\perp h_{\rm res}$. Then the described procedure gives

$$\vec{\boldsymbol{C}}(z) = C_0 \begin{pmatrix} e^{-(\hat{d}-\hat{z})} \\ 0 \\ -s_0\,\hat{z}\,e^{-(\hat{d}+\hat{z})} \\ -s_0\,e^{-(\hat{d}+\hat{z})} \end{pmatrix}, \qquad C_0 = \frac{\alpha \hat{p}_f}{H_d}\frac{k_\perp h_{\rm res}}{2}. \tag{29}$$

Substituting eq. (29) into eq. (12) one obtains expressions for elastic deformations above the reservoir,

$$\nabla \cdot \hat{\vec{\boldsymbol{u}}}_\perp = C_0 \left[e^{-|\hat{d}-\hat{z}|} + s_0\,\mu\, e^{-(\hat{d}+\hat{z})} - s_0\,\hat{z}\, e^{-(\hat{d}+\hat{z})} \right], \tag{30}$$

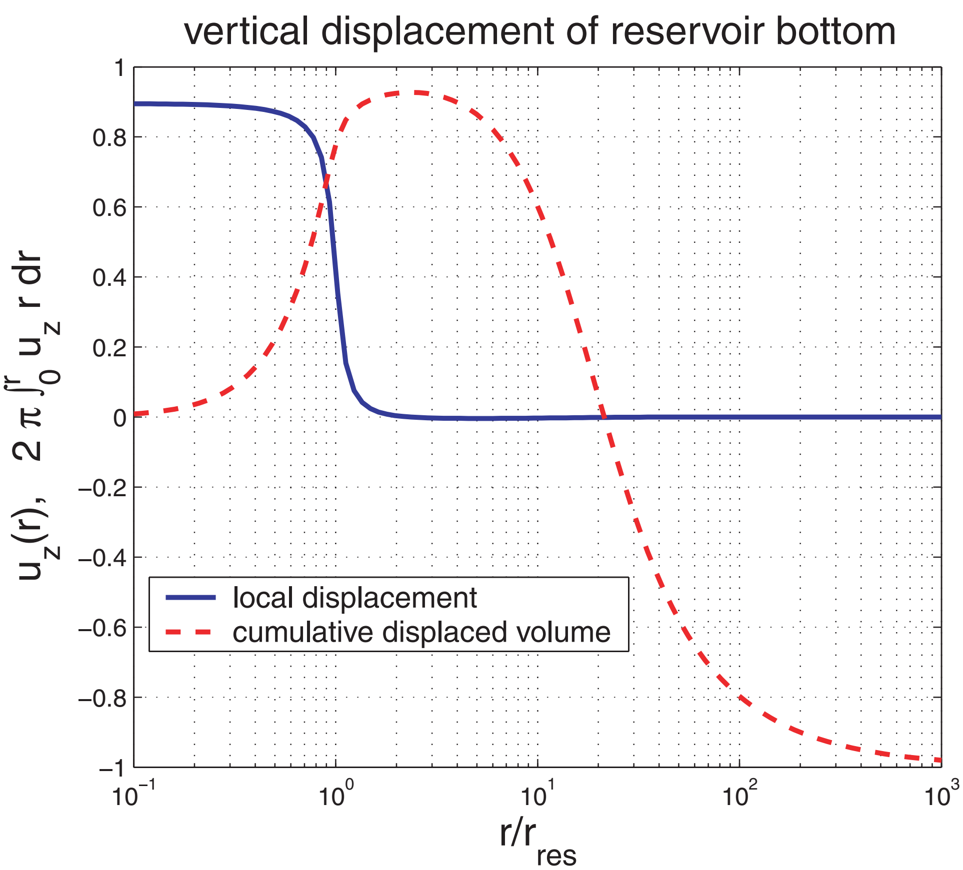

Figure 1. Vertical displacement $u_z(r)$ and cumulative displaced volume $V_z(r)$ below a uniformly depleted thin cylindrical reservoir with $d/r_{\rm res} = 10$ and $\nu = 0.25$ in a uniform half-space. Data are given at depth $z = 1.01d$. The normalizations $u_z \to -u_z(r)/\bar{u}_z$ and $V_z \to -V_z(r)/[2\pi r_{\rm res}^2(1-2\nu)\bar{u}_z]$ are used, so that positive values correspond to upward displacements.

$$\hat{\tau}_{zz} = 2C_0 N\left[-e^{-|\hat{d}-\hat{z}|} + \frac{s_0}{2}\, e^{-(\hat{d}+\hat{z})} + s_0\,\hat{z}\, e^{-(\hat{d}+\hat{z})}\right], \tag{31}$$

$$\frac{\nabla\cdot\hat{\boldsymbol{\tau}}_{\perp z}}{k_\perp} = 2C_0 N\left[e^{-|\hat{d}-\hat{z}|} - \frac{s_0}{2}\, e^{-(\hat{d}+\hat{z})} + s_0\,\hat{z}\, e^{-(\hat{d}+\hat{z})}\right], \tag{32}$$

$$k_\perp \hat{u}_z = C_0\left[-e^{-|\hat{d}-\hat{z}|} - s_0\,\mu\, e^{-(\hat{d}+\hat{z})} - s_0\,\hat{z}\, e^{-(\hat{d}+\hat{z})}\right]. \tag{33}$$

Elastic deformations below the reservoir are found similarly. They are given by the same relations as eqs (30)–(33) with the difference that the first terms in right sides of eqs (32) and (33) change signs. Using eqs (30)–(33) one can determine deformations for arbitrary pressure profiles. The solution corresponding to a delta-functional pressure drop is called the nucleus of strain solution. For the case of a half-space it has been found by Mindlin & Cheng (1950) and Sen (1951) and for the case of bi-materials by Rongved (1955).

It is convenient to interpret above equations in terms of the Hankel transform. If the pore pressure is equal to unity inside a disc with the radius $r_{\rm res}$ and vanishes outside this disc, then its Hankel transform scales as $k_\perp \hat{p}_f(k_\perp) = (2\pi r_{\rm res}) J_1(k_\perp r_{\rm res})$. The inverse Hankel transform of eqs (30)–(33) is obtained by multiplying them on $\hat{J}_0(k_\perp r) k_\perp \hat{p}_f(k_\perp)$ and integrating over $k_\perp$. This immediately leads to Geertsma's expressions. Geertsma (1973) has described a cylindrical reservoir by integrating the nucleus of strain solution over a disc area. We see however, that it is easier to reproduce his results directly from eqs (30) to (33). To recover the nucleus of strain solution, we consider the limit $k_\perp r_{\rm res} \ll 1$. In this limit $J_1(k_\perp r_{\rm res}) \to k_\perp r_{\rm res}/2$ and $\hat{p}_f = \pi r_{\rm res}^2$. The inverse Hankel transforms of eqs (30)–(33) contain integrals with products of Bessel functions and exponents, which are calculated analytically (Prudnikov *et al.* 1986),

$$\int_0^\infty k_\perp^n\, J_\beta(k_\perp r)\, e^{-k_\perp z}\, dk_\perp = \frac{(-1)^n}{r^\beta}\,\frac{\partial^n}{\partial z^n}\,\frac{(R-z)^\beta}{R}. \tag{34}$$

Here, $R = (r^2 + z^2)^{1/2}$ and $z > 0$. Deformations of a half-space are obtained by using eq. (34) and taking $s_0 = 2$. Notice, that s_0 appears as a multiplicative factor in front of all terms proportional to $\exp[-(\hat{d}+\hat{z})]$. In the Mindlin and Cheng formalism, which has been also used by Geertsma, such terms represent an 'image' nucleus. Consequently, expressions by Mindlin and Cheng and by Geertsma, become applicable to bi-material formations if one multiplies contributions of the image nuclei on $s_0/2$.

4.2 Stress above a rectangular plate

To verify the method, we calculate numerically the distribution of the vertical stress near a rectangular plate. This example admits an analytical solution (Hu 1989), which is used as a benchmark. Hu obtained this solution for thermoelastic deformations. However, it is equally applicable to the poroelastic case, because, as has been discussed by Geertsma (1973), the two above cases are mathematically identical.

Majority of studies of layered media uses Fourier or Hankel transforms in space domain (Peirce & Siebrits 2001a; Wang & Kümpel

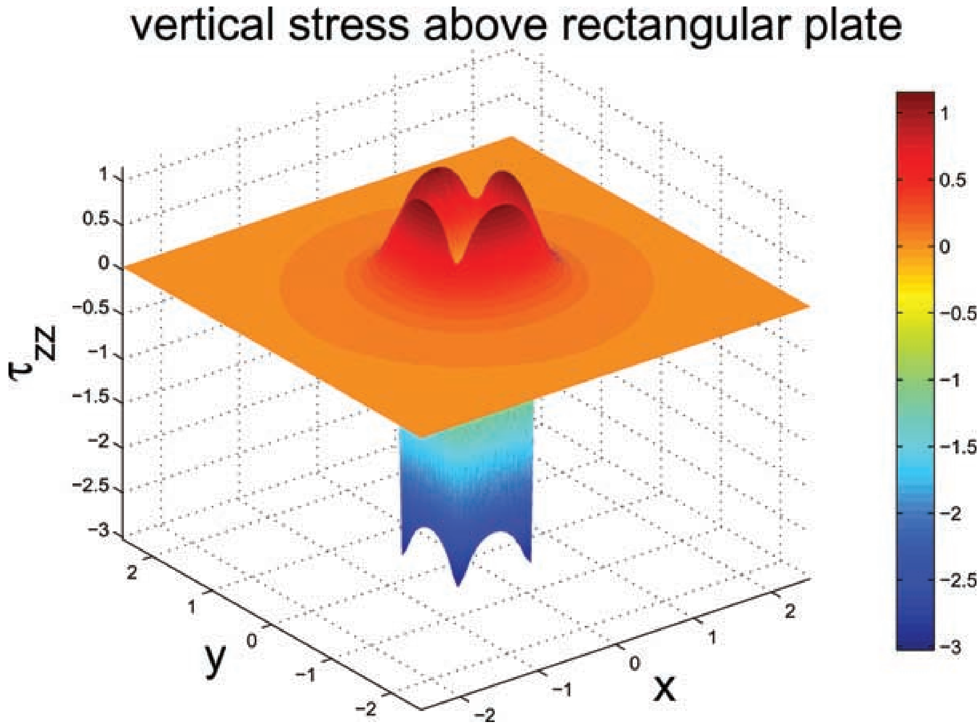

Figure 2. Normalized vertical stress τ_{zz} at plane $z = 0.99$ induced by a rectangular plate with a uniform pressure excess. The plate with dimensions $1 \times 1 \times 0.2$ is located at distance 1 below an infinitely rigid material.

2003; Fukahata & Matsu'ura 2005). Inverse transforms require evaluation of infinite integrals. Although this does not usually cause problems, one can also proceed in a different way. Namely, one can formulate the problem in terms of a discrete Fourier transform. This is especially convenient for a quick evaluation, when a high accuracy of calculations is not required. Subroutines with fast Fourier transform (FFT) are included in standard packages like MATLAB. They can be used directly, and one does not need additional pieces of code for numerical integration.

To adjust the described procedure to FFT, one should have in mind that the squared horizontal wave vector has been introduced as an eigenvalue of the Laplacian operator. The second derivative of a function g in finite differences is equal to $g''_n = (g_{n+1} - 2g_n + g_{n-1})/\Delta^2$. Here, n enumerates gridpoints and Δ is the distance between neighbouring points on the grid. For functions of the form $g_n \propto \exp\,(inkL)$ the above expression gives $g''_n = -(4g_n/\Delta^2)\sin^2(kL/2)$. Consequently, the wave vector $k_\perp$ is expressed through parameters of a discrete Fourier transform as $k_\perp^2 = (4/\Delta^2)\,[\sin^2(k_xL_x/2) + \sin^2(k_yL_y/2)]$. For clarity we have assumed that the spatial grid is squared.

Fig. 2 shows distribution of the vertical stress τ_{zz} in a horizontal plane above a rectangular plate (reservoir), which has been calculated in accordance with the described procedure. The stress is normalized on the value $\alpha p_f h_{\mathrm{res}} N/H_d$. The plate has a rectangular cross-section with length of 1 (in arbitrary units), thickness of 0.2, and it is buried at depth of 1, which is distance form the interface to the plate top. The plane, where the stress is calculated, is located at the distance 0.01 from the plate top. We have chosen such a small distance, because it allows to observe small scale harmonics of the deformation, which decay exponentially at larger distances. We have specified the upper layer to be infinitely rigid, so that the displacement vanishes at the interface. The calculations have been made by applying FFT on a square domain, whose size is five times larger than the plate size. The domain has been split in 64×64 cells. The pore pressure profile $\hat{p}_f$ has been generated purely numerically. Namely, we set $p_f = 1$ at gridpoints with $|x| < 1$ and $|y| < 1$, and then took the FFT of the resulting distribution.

Fig. 3 shows the same vertical stress along the line $y = 0$. It also compares the numerical result with the outcome of analytical formula of Hu (1989), which confirms the accuracy of calculations.

5 DISCUSSION AND CONCLUSIONS

The main conclusion of this paper is that the reflectivity method can be formulated in terms of LU matrix decompositions. Decomposition of the transfer matrix (6) and (7) gives transmission and reflection matrices. Decomposition of the scattering matrix (10) gives block-elements of the transfer matrix. The formula for LU decomposition of matrix products gives recursion relations (8) and (9) for transmission and reflection matrices.

The reflectivity method in the above formulation becomes a purely algebraic scheme, and it is applicable to arbitrary systems of differential equations. In particular, it can be effectively used to calculate static elastic deformations of a layered medium. Such deformations are governed by degenerate matrices, which cannot be analysed within the framework of the standard approach. To apply the reflectivity method to equilibrium cases, one uses the Jordan decomposition of the governing matrix $\hat{\mathbf{A}}$ in eq. (1) and expand the Jordan matrix (2) in the form of eq. (11). This separates modes with different exponential behaviour, which makes the procedure numerically stable.

The computational procedure admits different realizations, depending on the treatment of the transfer matrix $\boldsymbol{Q}(b,\,a) = \boldsymbol{M}^{-1}(b)\cdot\boldsymbol{M}(a)$ through interfaces. Using LU decomposition of $\boldsymbol{Q}(b,\,a)$ on obtains a scheme of the Kennett type (Kennett 1983). If the

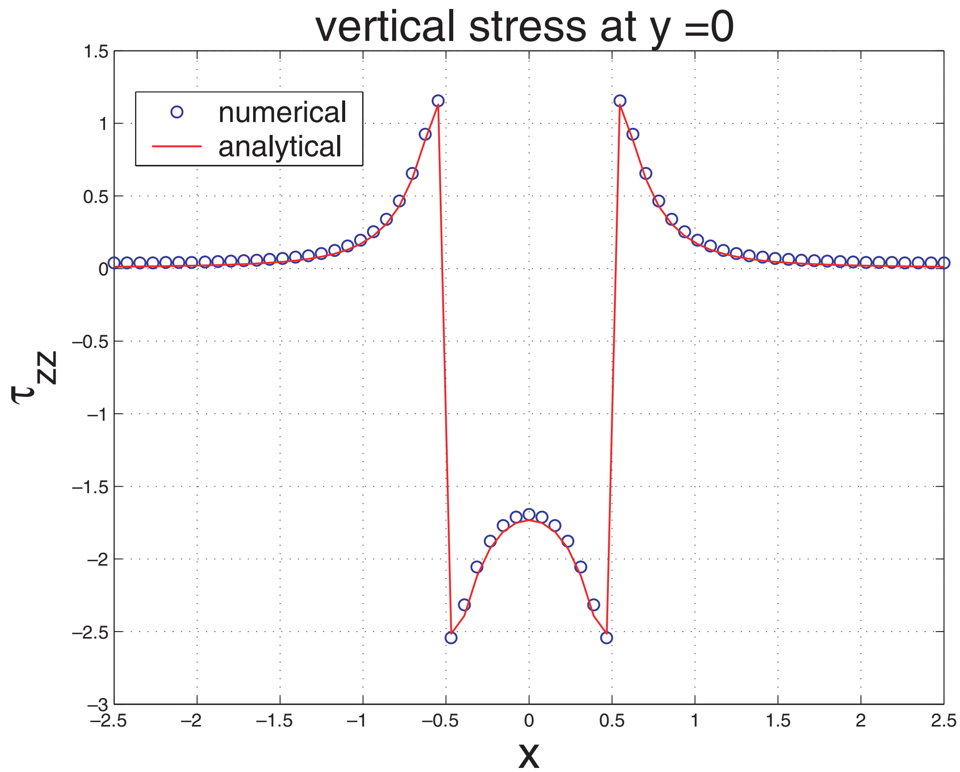

Figure 3. Data from Fig. 2 (open circles) are compared with analytical formula (solid curve) along the axis $y = 0$.

matrices $\boldsymbol{M}^{-1}(b)$ and $\boldsymbol{M}(a)$ are decomposed individually, one has a generalization of the method proposed by Rokhlin & Wang (2002). We have used the first realization in Sections 3 and 4. Individual decomposition of $\boldsymbol{M}^{-1}(b)$ and $\boldsymbol{M}(a)$ decreases speed of computations. This drawback is compensated by a higher clarity of the algorithm. As a result, the second realization may be preferable in analysis of systems containing more than four equations (see Appendix A).

In most practical cases, the governing equations can be derived in the coordinate space until the last step, where an integral or discrete transform is used. The only property of the transform, which is required for our analysis, is that it converts the action of the Laplacian operator in the horizontal plane $\nabla_\perp^2$ into multiplication on the 'wave vector' $-k_\perp^2$. Solutions are written in a general form, like those given by eqs (30)–(33), and the transform needs to be specified only when the concrete calculations are carried out. This gives the method a large flexibility. Appropriate choice of the transform simplifies both derivation of analytical formulas (Section 4.1), and numerical simulations (Section 4.2).

In this paper, we have analysed so-called hydrostatic deformations with a potential external force. The same procedure can be used to investigate arbitrary external forces. The difference with the described calculations is that one should appropriately modify the solution inside the reservoir layer and the matching conditions at the reservoir boundaries.

ACKNOWLEDGMENTS

I appreciate fruitful discussions with Stephen Bourne, Paul Hatchell, Paul Hofstra, and Rick Wentinck. Alexei Savitski provided references (Peirce & Siebrits 2001a,b), which were very helpful to get an overview of the subject.

REFERENCES

Ben-Menahem, A. & Singh, S.J., 1968. Radiation pattern of surface waves from point sources in a multi-layered medium, *Bull. seism. Soc. Am.,* **58,** 1519–1572.

Benitez, F.G. & Rosakis, A.J., 1987. Three-dimensional elastostatics of a layer and a layered medium, *J. Elasticity,* **18,** 3–50.

Biot, M.A., 1956. Theory of propagation of elastic waves in a fluid saturated porous solid i. low frequency range, *J. acoust. Soc. Am.,* **28,** 168–178.

Bonafede, M. & Rivalta, E., 1999. The tensile dislocation problem in a layered elastic medium, *Geophys. J. Int.,* **134,** 341–356.

Booth, D.C. & Crampin, S., 1983. The anisotropic reflectivity technique: Theory, *Geophys. J. R. astr. Soc.,* **72,** 755–766.

Bufler, H., 1971. Theory of elasticity of a multilayered medium, *J. Elasticity,* **1,** 125–143.

Chapman, C., 2004. *Fundamentals of Seismic Wave Propagation*, Cambridge University Press, Cambridge.

Frenkel, J., 1944. On the theory of seismic and seisoelectric phenomena in most soil, *J. Physics,* **8,** 230–241.

Fryer, G.J. & Frazer, L.N., 1984. Seismic waves in stratified anisotropic media, *Geophys. J. R. astr. Soc.,* **78,** 691–710.

Fuchs, K., 1968. The reflection of spherical waves from transition zones with arbitrary depth-dependent elastic moduli and density, *J. Phys. Earth,* **16**(Special Issue), 27–41.

Fuchs, K. & Müller, G., 1971. Computation of synthetic seismograms with the reflectivity method and comparison with observations, *Geophys. J. R. astr. Soc.,* **23,** 417–433.

Fukahata, Y. & Matsu'ura, M., 2005. General expressions for internal deformation fields due to a dislocation source in multilayered half-space, *Geophys. J. Int.,* **161,** 507–521.

Geertsma, J., 1973. Land subsidence above compacting oil and gas reservoir, *J. Petrol. Technol.,* **25,** 734–744.

Gilbert, F. & Backus, G.E., 1966. Propagator matrices in elastic wave and vibration problem, *Geophysics,* **31,** 326–332.

Haines, S.S., Pride, S.R., Klemperer, S.L. & Biondi, B., 2007. Seismoelectric imaging of shallow targets, *Geophysics,* **72,** G9–G20.

Haskell, N.A., 1953. The dispersion of surface waves in multilayered medium, *Bull. seism. Soc. Am.,* **43,** 17–34.

Haskell, N.A., 1964. Radiation pattern of surface waves from point sources in a multi-layered medium, *Bull. seism. Soc. Am.,* **54,** 377–393.

He, Y.M., Wang, W.M. & Yao, Z.X., 2003. Static deformation due to shear and tensile faults in a layered half-space, *Bull. seism. Soc. Am.,* **93,** 2253–2263.

Hu, S.M., 1989. Stress from a parallelepipedic thermal inclusion in a semispace, *J. Appl. Phys.,* **66,** 2741–2743.

Jovanovich, D.B., Husseini, M.I. & Chinnery, M.A., 1974. Elastic dislocations in a layered half space—i. basic theory and numerical methods, *Geophys. J. R. astr. Soc.,* **39,** 205–217.

Kennett, B.L.N., 1974. Reflections, rays, and reverberations, *Bull. seism. Soc. Am.,* **64,** 1685–1696.

Kennett, B.L.N., 1983. *Seismic Wave Propagation in Stratified Media*, Cambridge University Press, Cambridge.

Kennett, B.L.N. & Kerry, N.J., 1979. Seismic waves in a stratified half-space, *Geophys. J. R. astr. Soc.,* **57,** 557–584.

Linkov, A.M. & Filippov, N.A., 1991. Difference equations approach to the analysis of layered systems, *Meccanica,* **26,** 195–209.

Ma, X.Q. & Kusznir, N.J., 1992. 3D subsurface displacement and strain fields for faults and fault arrays in layered elastic half-space, *Geophys. J. Int.,* **111,** 542–558.

Maier, G. & Novati, G., 1986. On boundary element-transfer matrix analysis of layered elastic systems, *Engrg. Anal.,* **3,** 208–216.

Maier, G. & Novati, G., 1987. Boundary element elastic analysis of layered elastic soils by a successive stiffness method, *Int. J. Numer. Meth. Engrg.,* **11,** 435–447.

Matsu'ura, M. & Sato, R., 1975. Static deformations due to the fault spreading over several layers in a multi-layered medium. Part ii: strain and tilt, *J. Phys. Earth,* **23,** 1–29.

Mindlin, R.D. & Cheng, D.H., 1950. Thermoelastic stress in the semi-infinite solid, *J. Appl. Phys.,* **21,** 931–933.

Müller, G., 1985. The reflectivity method: a tutorial, *J. Geophys.,* **58,** 153–174.

Pan, E., 1997. Static Green's functions in multilayered half spaces, *Applied Math. Modeling,* **21,** 509–521.

Pan, E., 2001. Static Green's functions in multilayered half spaces, *Applied Math. Modeling,* **21,** 509–521.

Pan, E., 2003. Three-dimensional fundamental solutions in multilayered piezoelectric solids, *Chinese J. Mech. Ser. A,* **19,** 127–132.

Peirce, A.P. & Siebrits, E., 2001a. The scaled flexibility matrix method for the efficient solution boundary value problems in 2D and 3D elastic media, *Fracture,* **190,** 5935–5956.

Peirce, A.P. & Siebrits, E., 2001b. Uniform asymptotic approximations for accurate modeling of cracks in layered elastic media, *Int. J. Fractures,* **110,** 205–239.

Pride, S., 1994. Governing equations for the coupled electromagnetics and acoustics of porous media, *Phys. Rev. B,* **50,** 15 678–15 696.

Pride, S.R. & Haartsen, M.W., 1996. Electroseismic wave properties, *J. acoust. Soc. Am.,* **100,** 1301–1315.

Pride, S.R., Tromeur, E. & Berryman, J.G., 2002. Biot slow-wave effects in stratified rock, *Geophysics,* **67,** 271–281.

Prudnikov, A., Brychkov, Y.A. & Marichev, O.I., 1986. *Integrals and Series,* Vol. 2, Special Functions, Gordon and Breach, New York.

Revil, A., Schwaeger, H., Cathles, L.M. & Manhardt, P.D., 1999. Streaming potential in porous media 2. theory and application to geothermal systems, *J. geophys. Res.,* **104,** 20 033–20 048.

Rokhlin, S.I. & Wang, L., 2002. Stable recursive algorithm for elastic wave propagation in anisotropic media: stiffness matrix method, *J. acoust. Soc. Am.,* **112,** 822–834.

Rongved, L., 1955. Force interior to one of two joined semi-infinite solids, in *2nd Midwestern Conf. Solid Mech.,* Vol. 129, pp. 1–13, ed. Bogdanoff, J.L., Purdue University, Indiana, Res. Ser.

Roth, F., 1990. Subsurface deformations in a layered half-space, *Geophys. J. Int.,* **103,** 147–155.

Rundle, J.B., 1980. Static elastic-gravitational deformation of a layered half space by point coupled sources, *J. geophys. Res.,* **85,** 5355–5363.

Rundle, J.B., 1981. Vertical displacements from a rectangular fault in a layered elastic gravitational media, *J. Phys. Earth,* **29,** 173–196.

Rundle, J.B., 1982. Viscoelastic-gravitational deformation by a rectangular thrust fault in a layered earth, *J. geophys. Res.,* **87,** 7787–7796.

Sato, R., 1971. Crustal deformation due to dislocation in a multi-layered medium, *J. Phys. Earth,* **19,** 31–46.

Sato, R. & Matsu'ura, M., 1973. Static deformations due to the fault spreading over several layers in a multi-layered medium. part i: displacement, *J. Phys. Earth,* **21,** 227–249.

Savage, J.C., 1998. Displacement field for an edge dislocation in a layered half-space, *J. geophys. Res.,* **103,** 2439–2446.

Segall, P., 1992. Induced stresses due to fluid extraction from axisymmetric reservoirs, *Pageoph.,* **13,** 535–560.

Sen, B., 1951. Note on stresses produced by nuclei of thermo-elastic strain in a semi-infinite elastic solid, *Quatr. Appl. Math.,* **8,** 365–369.

Singh, S.J., 1970. Static deformation of a multilayered half-space by internal sources, *J. geophys. Res.,* **75,** 3257–3263.

Singh, S.J. & Singh, M., 2004. Deformation of a layered half-space due to a very long tensile fault, *Proc. Indian Natl. Acad. Sci.,* **113,** 235–246.

Singh, S.J., Punia, M. & Kumari, G., 1997. Deformation of a layered half-space due to a very long dip-slip fault, *Proc. Indian Natl. Acad. Sci.,* **63a,** 225–240.

Takeuchi, H. & Saito, M., 1972. Seismic surface waves, in *Methods of Computational Physics,* Vol. 11, Methods of Computational Physics, ed. Bolt, B.A., Academic Press, New York.

Thompson, A.H. *et al.*, 2007. Field tests of electroseismic hydrocarbon detection, *Geophysics,* **72,** N1–N9.

Thompson, R.R., 1936. The seismic electric effect, *Geophysics,* **1,** 327–335.

Thomson, W.T., 1950. Transmission of elastic waves through a stratified medium, *J. Appl. Phys.,* **21,** 89–93.

Ursin, B., 1983. Review of elastic and electromagnetic wave propagation in horizontally layered media, *Geophysics,* **48,** 1063–1081.

Wang, R., 1999. A simple orthonormalization method for stable and efficient computation of Green's function, *Bull. seis. Soc. Am.,* **89,** 733–741.

Wang, R. & Kümpel, H.-J., 2003. Poroelasticity: efficient modelling of strongly coupled, slow deformation processes in a multilayered half-space, *Geophysics,* **68,** 705–717.

Wang, R., Martín, F.L. & Roth, F., 2003. Computation of deformation induced by earthquakes in a multi-layered elastic crust-Fortran programs EDGRN/EDCMP, *Comput. Geosci.,* **29,** 195–207.

Xie, X.B. & Yao, Z.X., 1989. A generalized reflection-transmission coefficient matrix method to calculate static displacement field of a dislocation source in a stratified half-space, *Chinese J. Geophys.,* **32,** 191–205.

Yang, B. & Pan, E., 2002. Efficient evaluation of three-dimensional green's functions in anisotropic elastostatic multilayered composites, *Engng. Anal. Bound. Elements,* **26,** 355–366.

Zhao, S., Müller, R.D., Takahashi, Y. & Kaneda, Y., 2004. 3D finite element modeling of deformation and stress associated with faulting: effect of inhomogeneous crustal structures, *Geophys. J. Int.,* **157,** 629–644.

Zhu, L. & Rivera, L., 2002. A note on the dynamic and static displacements from a point source in multilayered media, *Geophys. J. Int.,* **148,** 619–627.

APPENDIX A: ELECTROKINETIC EQUILIBRIUM

The idea to use electrokinetic and electroseismic signals in geophysical prospecting has a long history (Thompson 1936; Frenkel 1944). These signals are very weak, however with the development of technology their measurement becomes feasible, see (Haines *et al.* 2007; Thompson *et al.* 2007) and references therein. A detail derivation of poroelastic equations in presence of electrokinetic coupling is given by Pride (1994). In subsequent papers, Pride and co-authors have found corresponding eigenmodes (Pride & Haartsen 1996) and have applied the reflectivity method (Pride *et al.* 2002) to study propagation of electroseismic waves. We apply the formalism developed in this paper to analyse the quasi-stationary limit of electrokinetic equations, where the governing matrix is degenerate. This analysis provides a rigorous theoretical basis for modelling of streaming potentials induced by ground fluid flows (see, e.g. Revil *et al.* 1999).

A1 Physical model

The coupled, low-frequency electrokinetic motion of the solid frame and pore fluid (Pride 1994) is described by a set of equations consisting of the bulk momentum balance,

$$0 = \nabla\cdot \overleftrightarrow{\boldsymbol{\tau}} + \vec{\boldsymbol{f}}, \tag{A1}$$

the fluid filtration equation,

$$\frac{\eta}{\kappa}\frac{\partial \vec{\boldsymbol{w}}}{\partial t} = -\nabla p_f + \frac{\eta}{\kappa}\Pi\ \nabla\phi + \frac{\eta}{\kappa}\vec{\boldsymbol{q}}, \tag{A2}$$

and the generalized Ohm's law,

$$\vec{\boldsymbol{j}} = -\sigma\nabla\phi + \Pi\nabla p_f. \tag{A3}$$

Here, $\overleftrightarrow{\boldsymbol{\tau}}$ is the total stress tensor, $\vec{\boldsymbol{w}}$ is the Darcy filtration displacement (relative displacement of the pore fluid with respect to the solid frame multiplied by the media porosity), p_f is the excess pore pressure, ϕ is the electrostatic potential, η is the fluid viscosity, κ and σ are the medium permeability and conductivity, Π is the electrokinetic coupling coefficient, and $\vec{\boldsymbol{F}}$ represents an external force that pumps the pore fluid pressure. Eqs (A1) and (A2) are supplemented by constitutive relations

$$\tau_{jk} = H_d\nabla\cdot\vec{\boldsymbol{u}}\,\delta_{jk} + 2N\left(e_{jk} - \nabla\cdot\vec{\boldsymbol{u}}\,\delta_{jk}\right) - \alpha p_f, \tag{A4}$$

$$p_f = -H_f\left(\alpha\nabla\cdot\vec{\boldsymbol{u}} + \nabla\cdot\vec{\boldsymbol{w}}\right), \tag{A5}$$

and the current closure condition $\nabla\cdot\vec{\boldsymbol{j}} = 0$ (it follows from the Maxwell equation $\vec{\boldsymbol{j}} \propto \nabla\times\vec{\boldsymbol{B}}$), where $\vec{\boldsymbol{u}}$ is the bulk displacement, e_{jk} is the strain tensor, α, N, H_d and H_f are Biot parameters characterizing elastic properties of the medium. Biot parameters are expressed through compression moduli of the solid K_s, of the drained matrix K_d, and of the pore fluid K_f as through porocity φ and

$$\alpha = 1 - \frac{K_d}{K_s},\quad H_d = K_d + \frac{4}{3}N,\quad H_f^{-1} = \frac{\alpha-\varphi}{K_s} + \frac{\varphi}{K_f}. \tag{A6}$$

The effective shear modulus N is assumed to be the same as the shear modulus of the solid material.

A2 First-order system

Above equations are split in two independent systems, which contain first-order z-derivatives. The first of these systems is 8-D, and it describes the medium response on irrotational sources,

$$\frac{\partial}{\partial z}\begin{pmatrix}\nabla\cdot\vec{\boldsymbol{u}}_\perp\\ \tau_{zz}\\ p_f\\ \phi\end{pmatrix} = \mathbf{A}_{12}\cdot\begin{pmatrix}\nabla\cdot\vec{\boldsymbol{\tau}}_{\perp z}\\ u_z\\ \partial w_z/\partial t\\ j_z\end{pmatrix} + \begin{pmatrix}0\\ -f_z\\ \frac{\eta}{\gamma\kappa}q_z\\ \frac{\eta\Pi}{\gamma\kappa\sigma}q_z\end{pmatrix}, \tag{A7}$$

$$\frac{\partial}{\partial z}\begin{pmatrix}\nabla\cdot\vec{\boldsymbol{\tau}}_{\perp z}\\ u_z\\ \partial w_z/\partial t\\ j_z\end{pmatrix} = \mathbf{A}_{21}\cdot\begin{pmatrix}\nabla\cdot\vec{\boldsymbol{u}}_\perp\\ \tau_{zz}\\ p_f\\ \phi\end{pmatrix} - \begin{pmatrix}\nabla_\perp\cdot\vec{\boldsymbol{f}}\\ 0\\ \nabla_\perp\cdot\vec{\boldsymbol{q}}\\ 0\end{pmatrix}. \tag{A8}$$

Here,

$$\mathbf{A}_{12} = \begin{pmatrix}1/N & -\nabla_\perp^2 & 0 & 0\\ -1 & 0 & 0 & 0\\ 0 & 0 & -\frac{\eta}{\gamma\kappa} & -\frac{\eta\Pi}{\gamma\kappa\sigma}\\ 0 & 0 & -\frac{\eta\Pi}{\gamma\kappa\sigma} & -\frac{1}{\gamma\sigma}\end{pmatrix}, \tag{A9}$$

$$\mathbf{A}_{21} = \begin{pmatrix} -4N\left(1-\frac{N}{H_d}\right)\nabla_\perp^2 & -\left(1-\frac{2N}{H_d}\right)\nabla_\perp^2 & \frac{2\alpha N}{H_d}\nabla_\perp^2 & 0 \\ -\left(1-\frac{2N}{H_d}\right) & \frac{1}{H_d} & \frac{\alpha}{H_d} & 0 \\ -\frac{2\alpha N}{H_d}\frac{\partial}{\partial t} & -\frac{\alpha}{H_d}\frac{\partial}{\partial t} & \frac{\kappa}{\eta}\nabla_\perp^2 - \frac{1}{H_p}\frac{\partial}{\partial t} & -\Pi\nabla_\perp^2 \\ 0 & 0 & -\Pi\nabla_\perp^2 & \sigma\nabla_\perp^2 \end{pmatrix}, \tag{A10}$$

$\gamma = 1 - \eta\Pi^2/(\kappa\sigma)$, and $H_p = H_f(1+\alpha^2 H_f/H_d)^{-1}$. As has been explained by Pride & Haartsen (1996), the quantities in left sides of eqs (A7) and (A8) are continuous for open or even partially sealed interfaces. The second system is 4-D and it describes response on solenoidal sources. We do not consider it in what follows.

We use a coordinate transform, where the operators $\nabla_\perp^2$ and $\partial/\partial t$ are expressed through the transversal wave vector $k_\perp$ and the Laplace parameter s as $\nabla_\perp^2 \to -k_\perp^2$ and $\partial/\partial t \to s$. It is convenient to introduce the vectors

$$\begin{aligned} \vec{\psi}_u &= \left(\nabla\cdot\vec{\boldsymbol{u}}_\perp; i\tau_{zz}; -ip_f; \frac{k_\perp^2\phi}{s}\right)^T, \\ \vec{\psi}_d &= \left(\frac{\nabla\cdot\vec{\boldsymbol{\tau}}_{\perp z}}{k_\perp}; ik_\perp u_z; ik_\perp w_z; \frac{j_z}{k_\perp}\right)^T, \end{aligned} \tag{A11}$$

and the normalized vertical coordinate, $\hat{z} = k_\perp z$. Then eqs (A7) and (A8) reduce to, $\partial\vec{\psi}_u/\partial\hat{z} = \hat{\mathbf{A}}_{12}\cdot\vec{\psi}_d$ and $\partial\vec{\psi}_d/\partial\hat{z} = \hat{\mathbf{A}}_{21}\cdot\vec{\psi}_u$. Here,

$$\hat{\mathbf{A}}_{12} = \begin{pmatrix} \frac{1}{N} & -i & 0 & 0 \\ -i & 0 & 0 & 0 \\ 0 & 0 & \chi & i\xi\Pi \\ 0 & 0 & i\xi\Pi & -\frac{\xi}{\gamma\chi} \end{pmatrix}, \tag{A12}$$

$$\hat{\mathbf{A}}_{21} = \begin{pmatrix} 4N\left(1-\frac{N}{H_d}\right) & -i\left(1-\frac{2N}{H_d}\right) & -2i\frac{\alpha N}{H_d} & 0 \\ -i\left(1-\frac{2N}{H_d}\right) & \frac{1}{H_d} & -\frac{\alpha}{H_d} & 0 \\ -2i\frac{\alpha N}{H_d} & -\frac{\alpha}{H_d} & \frac{\lambda_p^2+\xi\Pi^2}{\chi} & i\Pi \\ 0 & 0 & i\Pi & -\frac{\chi}{\xi} \end{pmatrix}, \tag{A13}$$

and we have introduced the notations

$$\xi = \frac{\eta}{\gamma\kappa\sigma}, \quad \chi = \frac{\eta s}{\gamma\kappa k_\perp^2}, \quad \lambda_p^2 = 1 + \frac{\chi}{H_p}. \tag{A14}$$

Matrices $\hat{\mathbf{A}}_{12}$ and $\hat{\mathbf{A}}_{21}$ are symmetric, which simplifies further calculations.

A3 Fundamental solutions

Excluding $\vec{\psi}_d$, one obtains the second order equation for $\vec{\psi}_u$, which in the absence of sources reads as $\partial^2\vec{\psi}_u/\partial\hat{z}^2 = \hat{\mathbf{A}}_{12}\cdot\hat{\mathbf{A}}_{21}\cdot\vec{\psi}_u$, or

$$\frac{\partial^2}{\partial\hat{z}^2}\begin{pmatrix} \nabla\cdot\vec{\boldsymbol{u}}_\perp \\ i\tau_{zz} \\ -ip_f \end{pmatrix} = \begin{pmatrix} 3-\frac{2N}{H_d} & -\frac{i}{N}\left(1-\frac{N}{H_d}\right) & -\frac{i\alpha}{H_d} \\ -4iN\left(1-\frac{N}{H_d}\right) & -\left(1-\frac{2N}{H_d}\right) & -\frac{2\alpha N}{H_d} \\ -2iN\frac{\alpha\chi}{H_d} & -\frac{\alpha\chi}{H_d} & \lambda_p^2 \end{pmatrix}\cdot\begin{pmatrix} \nabla\cdot\vec{\boldsymbol{u}}_\perp \\ i\tau_{zz} \\ -ip_f \end{pmatrix}, \tag{A15}$$

and

$$\frac{k_\perp^2}{s}\frac{\partial^2\phi}{\partial\hat{z}^2} = \xi\Pi\left[2\frac{\alpha N}{H_d}\nabla\cdot\vec{\boldsymbol{u}}_\perp - \frac{i\alpha}{H_d}(i\tau_{zz}) + \frac{i}{H_p}(-ip_f)\right] + \frac{k_\perp^2}{s}\phi. \tag{A16}$$

Eigenvalues λ^2 of system (A15), (A16) are equal to

$$\lambda^2 = 1, \qquad \lambda^2 = \lambda_p^2. \tag{A17}$$

The first root in eq. (A17) has triple degeneration. Eq. (A17) shows that the eigenvalues of the original system are equal to $\lambda = \pm 1$ and $\lambda = \pm\lambda_p$, where λ_p is specified as the square root of λ_p^2 with the positive real part. The eigenvectors of eqs (A15) and (A16) are found straightforwardly,

$$\vec{\boldsymbol{m}}_1^{(u)} = \begin{pmatrix} 1 \\ -2iN \\ 0 \\ 0 \end{pmatrix}, \quad \vec{\boldsymbol{m}}_3^{(u)} = \begin{pmatrix} \bar{\alpha} \\ -2i\bar{\alpha}N \\ i\chi \\ -\xi\Pi \end{pmatrix}, \quad \vec{\boldsymbol{m}}_4^{(u)} = \begin{pmatrix} 0 \\ 0 \\ 0 \\ \xi \end{pmatrix}, \tag{A18}$$

where $\bar{\alpha} = \alpha H_f / H$ and $H = H_d + \alpha^2 H_f$ is the so-called bulk elastic modulus. Vectors (A18) represent solutions for $\vec{\psi}_u$. Solutions for $\vec{\psi}_d$ corresponding to eigenvalues with positive real parts are denoted as $\vec{m}_j^{(d)}$. From the equation $\lambda \vec{m}^{(d)} = \hat{\mathbf{A}}_{21} \cdot \vec{m}^{(u)}$ it follows

$$\vec{m}_1^{(d)} = \begin{pmatrix} 2N \\ -i \\ 0 \\ 0 \end{pmatrix}, \quad \vec{m}_3^{(d)} = \begin{pmatrix} 2\bar{\alpha}\lambda_p N \\ -i\bar{\alpha}\lambda_p \\ i\lambda_p \\ 0 \end{pmatrix}, \quad \vec{m}_4^{(d)} = \begin{pmatrix} 0 \\ 0 \\ i\xi\Pi \\ -\chi \end{pmatrix}. \tag{A19}$$

The fundamental vector $\vec{m}_2^{(u)}$ is a generalized eigenvector, which satisfies the condition $\hat{\mathbf{A}}_{12} \cdot \hat{\mathbf{A}}_{21} \cdot \vec{m}_2^{(u)} = \vec{m}_2^{(u)} + 2\vec{m}_1^{(u)}$,

$$\vec{m}_2^{(u)} = \left[\mu + \frac{\bar{\alpha}\beta}{2\chi}; \quad iN\left(1 - \frac{\bar{\alpha}\beta}{\chi}\right); \; i\beta; \; -\frac{\xi\Pi\beta}{\chi} \right]^T. \tag{A20}$$

Here,

$$\beta = 4\bar{\alpha}(1-\nu)N, \quad \mu = \frac{1}{2}\frac{H+N}{H-N} = \frac{3-4\nu}{2}, \tag{A21}$$

and $\nu = (1/2)(1 - 2N/H)/(1 - N/H)$ is the Poisson ratio. The corresponding vector $\vec{m}_2^{(d)}$ is equal to $\vec{m}_2^{(d)} = \hat{\mathbf{A}}_{21} \cdot \vec{m}_2^{(u)} - \vec{m}_1^{(d)}$, that is,

$$\vec{m}_2^{(d)} = \left[N\left(1 + \frac{\bar{\alpha}\beta}{\chi}\right); \quad i\mu\left(1 - \frac{\bar{\alpha}\beta}{2\chi}\right); \; \frac{i\beta}{\chi}; \; 0 \right]^T. \tag{A22}$$

Generalized eigenvector $\vec{m}_2$ is not determined uniquely, since one can add to it arbitrary linear combinations of $\vec{m}_1$ and $\vec{m}_4$. We have constructed $\vec{m}_2$ to satisfy the conditions $(\vec{m}_2^{(u)})^T \cdot \vec{m}_2^{(d)} = 0$ and $\vec{m}_2^T \cdot \vec{m}_4 = 0$.

A4 Transmissions and reflections

Combining above vectors one obtains the fundamental matrix $\boldsymbol{M}$. If we were dealing with non-degenerate governing matrix $\mathbf{A}$, then the eigenvector matrix $\boldsymbol{M}$ would have the form

$$\boldsymbol{M} = \begin{pmatrix} \boldsymbol{M}_u & \boldsymbol{M}_u \\ \boldsymbol{M}_d & -\boldsymbol{M}_d \end{pmatrix}, \tag{A23}$$

where

$$\boldsymbol{M}_{u,d} = \left(\vec{m}_1^{(u,d)} \quad \vec{m}_2^{(u,d)} \quad \vec{m}_3^{(u,d)} \quad \vec{m}_4^{(u,d)} \right). \tag{A24}$$

Form (A23) appears because eigenvectors associated with negative λ can be constructed from eigenvectors associated with positive λ by changing the sign of $\vec{m}^{(d)}$: $(\vec{m}_j^{(u)}, \vec{m}_j^{(d)}) \to (\vec{m}_j^{(u)}, -\vec{m}_j^{(d)})$, $j \neq 2$. This is not valid for the generalized eigenvector $\vec{m}_2$, where changing sign of λ results in the transformation $(\vec{m}_2^{(u)}, \vec{m}_2^{(d)}) \to (-\vec{m}_2^{(u)}, \vec{m}_2^{(d)})$. We notice that eqs (4) are invariant with respect to the transformation,

$$\boldsymbol{C} \to \boldsymbol{K} \cdot \boldsymbol{C}, \quad \boldsymbol{M} \to \boldsymbol{M} \cdot \boldsymbol{K}^{-1}, \quad \boldsymbol{J} \to \boldsymbol{K} \cdot \boldsymbol{J} \cdot \boldsymbol{K}^{-1}. \tag{A25}$$

If the transformation matrix $\boldsymbol{K}$ does not mix blocks of the Jordan matrix $\boldsymbol{J}$ with different λ, then the reflectivity algorithm is still applicable. We specify $\boldsymbol{K}$ as a diagonal matrix with unit elements except for the element (6, 6) that is equal to -1. Then the matrix $\boldsymbol{M}$ reduces to form (A23), which is used in the further analysis.

The LU decomposition of $\boldsymbol{M}$ and $\boldsymbol{M}^{-1}$ gives

$$\boldsymbol{M} = \begin{pmatrix} \boldsymbol{M}_u^{-1} & 0 \\ -\boldsymbol{M}_d \cdot \boldsymbol{M}_u^{-1} & \boldsymbol{I} \end{pmatrix}^{-1} \cdot \begin{pmatrix} \boldsymbol{I} & \boldsymbol{I} \\ 0 & -2\boldsymbol{M}_d \end{pmatrix}, \tag{A26}$$

and

$$\boldsymbol{M}^{-1} = \begin{pmatrix} 2\boldsymbol{M}_u & 0 \\ -\boldsymbol{I} & \boldsymbol{I} \end{pmatrix}^{-1} \cdot \begin{pmatrix} \boldsymbol{I} & \boldsymbol{M}_u \cdot \boldsymbol{M}_d^{-1} \\ 0 & \boldsymbol{M}_d^{-1} \end{pmatrix}. \tag{A27}$$

Similarly to the case of seismic waves (Ursin 1983; Fryer & Frazer 1984), the inverse matrices $\boldsymbol{M}_{u,d}^{-1}$ can be found without bulky calculations. The eigenvalue equation, $\boldsymbol{M}^{-1}\hat{\mathbf{A}} = \boldsymbol{J} \cdot \boldsymbol{M}^{-1}$, is written in index notations as

$$(M^{-1})_j^{\vartheta} \hat{A}_k^j = J_j^{\vartheta} (M^{-1})_k^j. \tag{A28}$$

In particular, taking $\vartheta = 1$ and $\vartheta = 2$ we obtain

$$(M^{-1})_j^2 \hat{A}_k^j = (M^{-1})_k^2, \quad (M^{-1})_j^1 \hat{A}_k^j = (M^{-1})_k^1 + (M^{-1})_k^2. \tag{A29}$$

Eqs (A28) and (A29) show that the first line of the matrix $\boldsymbol{M}^{-1}$ is a generalized eigenvector of the transposed matrix $\hat{\mathbf{A}}^T$ associated with the eigenvalue $\lambda = 1$, and the second line of $\boldsymbol{M}^{-1}$ is a generalized eigenvector of $\hat{\mathbf{A}}^T$ associated with $\lambda = 1$. Taking into account symmetry properties of the matrix $\hat{\mathbf{A}}$ one concludes,

$$\boldsymbol{M}_{u,d}^{-1} = \left(\vec{m}_2^{\star(d,u)}; \quad \vec{m}_1^{\star(d,u)}; \quad \vec{m}_3^{\star(d,u)}; \quad \vec{m}_4^{\star(d,u)} \right)^T. \tag{A30}$$

Here, $\vec{\boldsymbol{m}}_j^\star = g_j \vec{\boldsymbol{m}}_j$ for $j \neq 2$, $\vec{\boldsymbol{m}}_2^\star = g_2 \vec{\boldsymbol{m}}_2 + c_1 \vec{\boldsymbol{m}}_1 + c_3 \vec{\boldsymbol{m}}_3$, g_j and $c_{1,3}$ are some constants. In eq. (A20) we have used the freedom in determining the generalized eigenvector $\vec{\boldsymbol{m}}_2$ to provide the conditions $c_1 = c_3 = 0$. The constants g_j are given by the expressions

$$g_1 = g_2 = \frac{1}{4N(1-\nu)}, \quad g_3 = -\frac{1}{\lambda_p \chi}, \quad g_4 = -\frac{1}{\xi \chi}. \tag{A31}$$

Above equations contain all the necessary information to implement the reflectivity method for the electrokinetic equilibrium. Propagation through interfaces is considered as a combined translation $a \leftrightarrow b$ and $b \leftrightarrow c$. Here, points a and c lie above and below the interface, and b is a fictitious point between a and c. Applying composition rules (8), (9) to $\boldsymbol{M}(a)$ given by eq. (A26) and to $\boldsymbol{M}\,(c)$ given by eq. (A27), one can describe this propagation explicitely,

$$\boldsymbol{T}(a,c) = 2\left[\boldsymbol{M}_u^{-1}(c) \cdot \boldsymbol{M}_u(a) + \boldsymbol{M}_d^{-1}(c) \cdot \boldsymbol{M}_d(a)\right]^{-1}, \tag{A32}$$

$$\boldsymbol{R}(a,c) = \boldsymbol{I} - \boldsymbol{M}_d^{-1}(c) \cdot \boldsymbol{M}_d(a) \cdot \boldsymbol{T}(a,c). \tag{A33}$$